Catalysis and Synergism in the Reduction Smelting of Lead Sulfide with Carbon and Lime

The catalyzed direct reduction of lead sulfide with carbon and lime was investigated at several temperatures and under two different inert gas atmospheres. The catalyzed reduction kinetics were determined both with a nitrogen atmosphere and a helium-rich helium-nitrogen atmosphere. The reduction kinetics under the latter were decidedly superior to those under the former. The differences were interpreted in terms of faster diffusion rates in a helium medium and synergistic effects. The catalyst used was a ternay eutectic mixture (K, Li, $Na)_2CO_3$, which amounted to 2.5 wt. % of the PbS:4CaO:4C reaction mixture.

Y. K. RAO

and S. K. EL-RAHAIBY

Department of Materials Science and Engineering
University of Washington
Seattle, WA 98195

SCOPE

The effect of ambient atmosphere and the influence of temperature on the reduction smelting of lead sulfide with carbon and lime have been investigated in the temperature range 1,061 to 1,262 K. The experimental data are analyzed by means of a physicochemical model that envisions the Boudouard reaction ($C + CO_2 \rightarrow 2CO$) as the rate-controlling step for the overall reduction process. The intrinsic rate constant values were derived by the application of the model. The rate constant values for reduction under helium-rich helium-nitrogen atmospheres are systematically higher than those for reduction under nitrogen atmospheres. These differences were reconciled in terms of synergistc effects arising from the presence of the catalyst.

CONCLUSIONS AND SIGNIFICANCE

The addition of the ternary eutectic catalyst (K, Li, $Na)_2CO_3$ proved to be quite effective in promoting the reduction rates in the PbS:4CaO:4C mixtures in the temperature range 1,061 to 1,262 K. The catalyst was added in modest amounts, i.e., 2.5 wt. %, and is known to exist in a molten state at all the temperatures investigated. The extent of catalysis was found to be significantly influenced by the nature of the inert ambient atmosphere used. The reaction mechanism consisted of reduction, carbon gasification, and PbS vaporization steps with the middle step constituting the rate-limiting phenomenon. The intrinsic rate constant values for carbon gasification were obtained for two different atmospheres: $\log I_1 = 5.300 - 8{,}480\ T^{-1}$ for helium-rich helium-nitrogen atmospheres and $\log I_1 = 3.981 - 7{,}790\ T^{-1}$ for nitrogen atmospheres. The catalyst addition in conjunction with the ambient atmosphere, even though the latter is inert, produces a synergistic effect; that is, the catalyst is more effective in a helium-rich helium-nitrogen atmosphere as compared to a nitrogen atmosphere. This synergistic effect, expressed as a ratio of the intrinsic rate constants, has a value of 4.7 at 800°C, which rises to 6.0 at 1,000°C.

INTRODUCTION

The reduction of lead sulfide with carbon and lime is potentially an attractive route for producing lead. The overall reaction may be represented by

$$PbS(s) + CaO(s) + aC(s) = Pb(l) + CaS(s) + (2a - 1)CO + (1 - a)CO_2 \quad (A)$$

The proportion of CO to CO_2 in the ensuing gas phase depends on the temperature of reduction and the reactivity of the carbon reducing agent. Highly reactive forms of carbon or carbon-doped with catalyst tend to produce gases rich in CO.

In a recently concluded laboratory investigation (El-Rahaiby, 1983) an exhaustive study was made of the effects of a variety of experimental variables on the reduction kinetics of lead sulfide. Allied phenomena such as the vaporization of lead sulfide have also been studied by the present authors (El-Rahaiby and Rao, 1982). The purpose of this paper is to examine the role of the ambient atmosphere in the PbS-CaO-C system, especially when a catalyst is present. The present study extended from 788 to 989°C. Experiments were conducted under both a helium and a nitrogen atmosphere respectively, the results were compared, and the differences were interpreted in terms of synergistic effects stemming from the presence of the catalyst.

EXPERIMENTAL

The lead sulfide used in this study was supplied by Cerac Certified Chemicals (Milwaukee, WI); it had a minimum purity of 99.9% and was found to have an average particle size of 3.03 μm. The lime used had a minimum CaO content of 97% This analytical grade material was furnished by Mallinckrodt, Inc. (St. Louis, MO); its average particle size was 5.37 μm. Ultrapure graphite (UCP-1-325), with an average particle size of 0.94 μm, obtained from the Ultra Pure Carbon Corp. (Bay City, MI) was the reductant used in the present experiments.

Samples were prepared by mixing together the constituents PbS, CaO, and C in a 1:4:4 molar proportion in a manner similar to that described previously (El-Rahaiby and Rao, 1982). The entire preparation was carried out in a dry box, and its description has been published in the aforementioned paper. A portion of the three-component mixture was weighed into a 1.9 cm I.D. × 3.2 cm deep alumina crucible inside the dry box itself. The mixture was packed into the crucible by tapping repeatedly but without the application of any external pressure. The solids mixture in the final packed condition had a porosity in the range of 0.60 to 0.65. The crucible and its contents were placed in a desiccator and transferred out of the dry box.

The reduction kinetics were determined by the weight loss measurement technique using a conventional thermogravimetric apparatus. A schematic diagram of the setup used appeared in the publication mentioned earlier and so only a few details will be given here. The apparatus consisted of a vertical tube furnace that can be moved up and down over guide frames and an Ainsworth balance fixed firmly on a platform atop the furnace. The alumina crucible bearing the sample is suspended from the balance into the equitemperature zone (±3°C over 8 cm length) of the furnace. The balance housing is continuously flushed with purified nitrogen gas entering at the rate of 0.9 to 1.0 L (STP) per min. The main flow of N_2 or He entered through a gas distribution port located in the apparatus midway between the balance and the furnace. The rate of this flow was 2.5 L (STP) per min. Thus, in effect, the reduction was carried out under a pure N_2 atmosphere or a helium-rich He-N_2 atmosphere. The fraction of He in the He-N_2 mixtures was between 0.7 and 0.75.

The experimental procedure was essentially the same as that used in the case of the lead sulfide vaporization study reported recently. The reduction kinetics were determined under isothermal conditions. Both catalyzed and uncatalyzed reduction processes were investigated using the pure N_2 atmosphere. With the He-rich He-N_2 atmosphere, only the catalyzed reduction process was studied. The catalyst used is a ternary (K, Li, Na)$_2CO_3$ eutectic that has a particularly low melting point (399°C). The catalyst was made by prefusing together an equimolar mixture of K_2CO_3, Li_2CO_3, and Na_2CO_3 and crushing the solidified mass into a finely divided form. This fine powder was then added to the PbS:4CaO:4C mixture in the amount of 2.5 wt % of the total. All weighing and mixing were carried out inside the dry box to avoid moisture pickup by the lime.

With the He-rich He-N_2 atmosphere, the reduction kinetics of catalyzed mixtures were determined at eight different temperatures. The investigation with pure N_2 atmosphere was even more extensive; but only a limited portion of latter study will be considered here since a more detailed version is available elsewhere (Rao and El-Rahaiby, 1984).

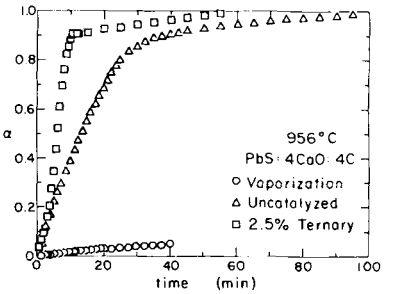

Figure 2. Reduction and vaporization kinetics under nitrogen atmosphere at 956°C.

RESULTS

The results with a N_2 atmosphere are shown in Figures 1, 2, and 3. The fractional reaction α vs. time t data shown were obtained from the weight loss measurements. For the reduction process

$$\alpha = \Delta W / \Delta W_{obs} \quad (1)$$

where

ΔW = weight loss sustained by the sample in time t
ΔW_{obs} = cumulative weight loss that corresponds to completion of reduction

The value of ΔW_{obs} was determined experimentally for each run; it can also be calculated from the stoichiometry of reaction A by assuming that CO is the sole gaseous product of reduction. One source of uncertainty in the observed weight loss is the possible loss of PbS vapor through vaporization, which, if left unaccounted for, may falsify the measured reduction kinetics. The vaporization was held in check by employing excess lime and excess carbon in the PbS/CaO/C mixtures. These large "excesses" ensure that the PbS vapor molecules have a negligible chance of escaping unreacted into the ambient atmosphere. By careful investigation, it was found that a mixture with the proportion PbS:4CaO:4C, i.e., with 300% excess CaO and C, respectively, is quite satisfactory in curtailing the PbS vapor loss (El-Rahaiby, 1983). Thus the weight loss observed here is a good indicator of the degree of reduction sustained by the mixture.

In Figures 1 to 3 there are also shown the α vs. t plots for vaporization from PbS:4CaO mixtures (El-Rahaiby and Rao, 1982). These are included for comparison. It is well to note that α in this case is obtained by dividing the weight loss at time t with the total

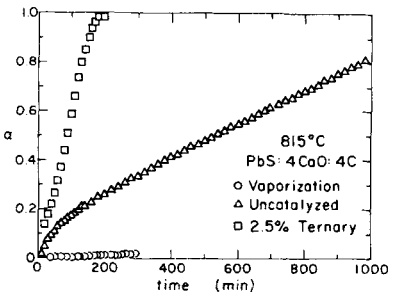

Figure 1. Reduction and vaporization kinetics under nitrogen atmosphere at 815°C.

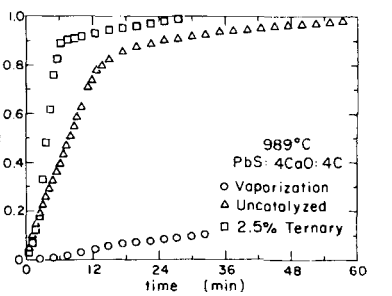

Figure 3. Reduction and vaporization kinetics under nitrogen atmosphere at 989°C.

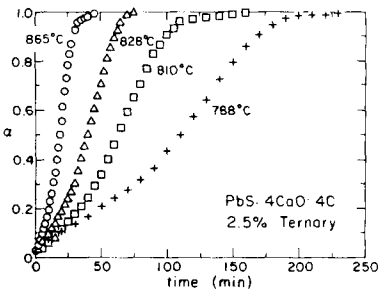

Figure 4. Kinetics of the catalyzed reduction process under helium-rich, helium-nitrogen atmospheres.

initial mass of PbS in the PbS:4CaO mixture. Thus, in this case, $\alpha = 1$ corresponds to complete vaporization of PbS. The kinetics of vaporization are decidedly slower than the kinetics of reduction.

Turning to Figure 1 we find that the addition of catalyst dramatically improves the rate of reduction under N_2 at 815°C. Similar catalytic effects are observed in Figures 2 and 3, which show the results under N_2 at 956 and 989°C, respectively. The extent of catalysis seems to diminish as the reduction temperature is increased from 815 to 989°C.

The reduction kinetics of the catalyzed mixtures reacted under a He-rich He-N_2 atmosphere are reported in Figures 4 and 5. A comparison of Figures 1 and 4 (the plot at 810°C) shows that the reduction occurs at a decidedly faster pace under the He-rich He-N_2 atmosphere. Figure 5 shows that the temperature influence is somewhat lessened in the case of catalyst-containing mixtures reacting under He-rich He-N_2 atmospheres especially when the temperatures exceed 900°C.

The α-t plots shown in Figures 1 to 5 exhibit a virtually constant-rate region in the middle. The rate constant for each experiment was determined from the slope of the α-t plot in this region. Thus

$$K = (d\alpha/dt), \text{ min}^{-1} \qquad (2)$$

Regression analysis of the α vs. t data in the constant-rate region provided the value of K for the particular temperature considered. Values of K thus obtained for the He-rich He-N_2 runs are listed in Table 1. Similar analysis was carried out with regard to the experiments done under pure N_2 atmosphere (Figure 6).

The experimental rate constant (K) data for both ambient atmospheres are presented in Figure 6 in the form of an Arrhenius plot. All these data are for the catalyst-bearing PbS:4CaO:4C mixtures. It is readily seen that reduction under the He-rich He-N_2 atmosphere is significantly faster than that under a pure N_2 atmosphere. Regression analysis of the log K vs. T^{-1} data yielded the following relationships:

$$\log K(\text{He}) = 9.143(\pm 0.356) - \frac{231.6(\pm 7.8)\ \text{kJ} \cdot \text{mol}^{-1}}{2.303\text{RT}}$$

$$\log K(\text{N}_2) = 9.153(\pm 0.315) - \frac{236.8(\pm 7.1)\ \text{kJ} \cdot \text{mol}^{-1}}{2.303\text{RT}}$$

The respective activation energies are 231.6 (±7.8) kJ·mol^{-1} for reduction under He-rich He-N_2 atmospheres and 236.8 (±7.1) kJ·mol^{-1} for reduction under pure N_2 atmosphere.

To gain insight into the mechanism of the reduction process, further work was done to ascertain the nature of the gas phase in the reduction system. Using a solid electrolyte (calcia-stabilized zirconia) galvanic cell, the reduction potential (or CO/CO_2 ratio) of the gas phase emanating from a mixture of PbS:4CaO:4C reacting under isothermal conditions was measured as a function of time. The details of this technique are given elsewhwere (El-Rahaiby, 1983) and only the results are considered here. The reduction potential (CO/CO_2) vs. time (t) data were converted into the ln (CO/CO_2) vs. α data using the α vs. t experimental data obtained earlier by the weight loss measurement technique. The results at 816 and 850°C are shown in Figures 7 and 8 respectively. Three different kinds of measurements are reported here: first, the uncatalyzed PbS:4CaO:4C mixtures reacting under a pure N_2 atmosphere; second, the catalyzed PbS:4CaO:4C mixtures reacting under a pure N_2 atmosphere; and third, the same mixtures reacting under a pure helium atmosphere. At both temperatures shown it is clear that the uncatalyzed reduction is associated with the smallest reduction potentials in the gas phase; this reduction potential remains virtually unchanged over the entire length of reduction. With the catalyzed mixtures reduced under N_2, the gas

Table 1. Experimental Data for the Catalyzed Reduction of PbS:4CaO:4C Mixtures Under He-Rich He-N_2 Atmosphere

Run No.	Temp. K	W°_T g	ΔW°_{obs} mg	θ	L cm	A_e cm^2	K(He) min^{-1}
E113	1,061	3.1420	201	0.639	0.744	2.950	0.0049
E114	1,083	2.9476	189	0.643	0.767	2.700	0.0105
E108	1,101	2.6961	164	0.614	0.577	3.036	0.0146
E107	1,138	2.9654	179	0.635	0.686	2.965	0.0308
E109	1,161	3.1455	191	0.612	0.688	2.950	0.0519
E110	1,190	3.4810	222	0.608	0.754	3.154	0.1138
E111	1,212	3.2710	204	0.615	0.719	2.965	0.1522
E112	1,247	3.4877	271	0.633	0.785	3.036	0.2362

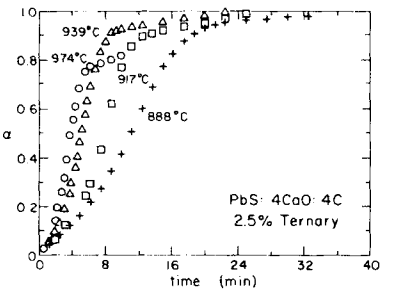

Figure 5. Kinetics of the catalyzed reduction process under helium-rich, helium-nitrogen atmospheres.

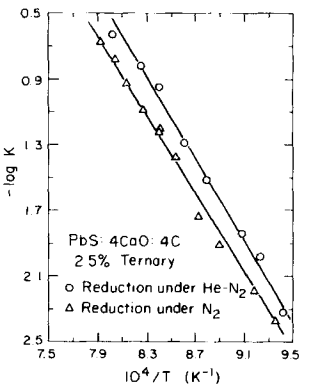

Figure 6. Arrhenius plots constructed using experimental rate constant data for catalyzed reaction under different atmospheres.

phase has much greater reduction potentials (as compared to uncatalyzed). However, the largest CO/CO_2 ratios are seen with reduction under the He atmosphere. Thus the superior reduction kinetics observed earlier with the He-rich He-N_2 atmosphere are neatly corroborated by the gas phase reduction potential data found here.

DISCUSSION

The faster kinetics observed with the He-rich He-N_2 atmosphere may be partly attributed to the larger values taken by the diffusivities of CO and CO_2 in a He-rich He-N_2. To facilitate the interpretation of the experimental data, a mechanistic model was formulated (Rao and El-Rahaiby, 1984), only the barest details of which are given here. The model assumes that the mechanism of reduction consists of a sequence of heterogeneous reaction steps as follows:

$$PbS(s) + CaO(s) + CO = Pb(l) + CaS(s) + CO_2 \quad (A1)$$

$$C(s) + CO_2 = 2CO \quad (A2)$$

$$PbS(s) = PbS(vapor) \quad (A3)$$

The last step in this sequence is the vaporization process that occurs parallel to the reduction process. Of the two remaining steps, the Boudouard (or the C-CO_2 reaction), i.e., reaction A2, appears to be the rate-controlling step in the uncatalyzed reduction process. With the catalyst, the rate of this reaction is enhanced but not enough to eliminate its rate-controlling characteristics. This is deduced from the fact that the activation energy for the reduction process decreases only slightly from 295.9 to 236.8 kJ·mol^{-1} upon the addition of the catalyst, whereas for a fully-catalyzed Boudouard reaction, the activation energy is but half of that for the uncatalyzed reaction.

The rate expression for the Boudouard reaction may be written as follows (Rao and Jalan, 1972; Walker et al., 1959):

$$-r_C = 0.5r_{CO} = \frac{I_1 P_{CO_2}}{1 + I_2 P_{CO} + I_3 P_{CO_2}} \quad (3)$$

where r_C, the rate of carbon gasification, is expressed in gmol/g of C/s. Of the total CO(g) generated by the Boudouard reaction, let us suppose that a fraction β is utilized in the reduction reaction A1. It is well to note that a sizable fraction of CO(g) is simply unavailable for the purposes of reduction; this may be because of the pore diffusion of CO(g) away from the site of reduction. The net rate of formation of CO(g), R_{CO}, is given by

$$R_{CO} = \frac{(2 - 2\beta) I_1 \rho_C P_{CO_2}}{1 + I_2 P_{CO} + I_3 P_{CO_2}} \quad (4)$$

where R_{CO} is expressed in gmol/cm^3/s.

The gas phase within the pore spaces of the reaction mixture (PbS:4CaO:4C) contains CO_2(g), which, it may be noted, is produced by reaction A1 and a portion of it is simultaneously consumed by the Boudouard reaction. The net rate of production of CO_2(g) may be expressed as

$$R_{CO_2} = \frac{(2\beta - 1) I_1 \rho_C P_{CO_2}}{1 + I_2 P_{CO} + I_3 P_{CO_2}} \quad (5)$$

In addition, we need to consider the vaporization of solid lead sulfide during the reduction process. The mechanism of vaporization is considered to be essentially same as that discussed previously (El-Rahaiby and Rao, 1982).

Development of the Model

The reaction mixture was contained in a cylindrical crucible only the upper surface of which is open to the surrounding gas phase. In a setup such as this only diffusion in a single direction need be considered. The following mass conservation relations may be derived in the usual manner (El-Rahaiby, 1983):

$$\frac{D_1}{RT} \frac{\partial^2 P_{CO}}{\partial y^2} + \frac{(2 - 2\beta) I_1 \rho_C P_{CO_2}}{1 + I P_{CO_2}} = 0 \quad (6)$$

$$\frac{D_2}{RT} \frac{\partial^2 P_{CO_2}}{\partial y^2} + \frac{(2\beta - 1) I_1 \rho_C P_{CO_2}}{1 + I P_{CO_2}} = 0 \quad (7)$$

and

$$\frac{D_3}{RT} \frac{\partial^2 P_{PbS}}{\partial y^2} + k_f [1 - (P_{PbS}/K_e)] = 0 \quad (8)$$

The mass balance for the carbon present in the system provides

$$\frac{\partial \rho_C}{\partial t} + \frac{M_C I_1 \rho_C P_{CO_2}}{1 + I P_{CO_2}} - = 0 \quad (9)$$

In the foregoing relations, $I = I_3 + (I_2/r)$, where r is the CO_2/CO ratio of the gas phase. The measured values obtained with the galvanic cell technique were used in finding the most representative value of r (= CO_2/CO) for each experiment.

The initial and the boundary conditions are as follows:

(*i*) $\rho_C = \rho_C^\circ$ at $t = 0$
(*ii*) $(\partial P_i/\partial y) = 0$ at $y = 0$, where i = CO, CO_2, or PbS
(*iii*) $P_i = P_i^{(s)}$ at $y = L$, where i = CO, CO_2, or PbS

The partial pressure terms appearing in the boundary condition (iii) were determined from the experimental data.

By combining Eqs. 6 and 7, it is possible to derive the following expression for the utilization factor:

$$\beta = (2 + q)(2 + 2q)^{-1} \quad (10)$$

where $q = (D_1/rD_2)$, with D_1 and D_2 denoting the effective diffusivities of CO and CO_2, respectively.

The reduction process with the accompanying vaporization is adequately represented by the set of Eqs. 6, 7, 8, and 9, together

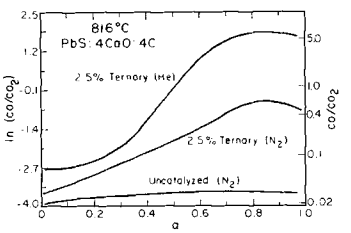

Figure 7. Reduction potentials (CO/CO_2) as function of fractional reduction at 816°C.

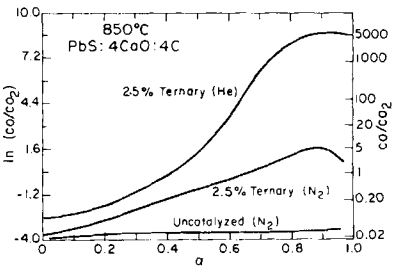

Figure 8. Reduction potentials (CO/CO_2) as function of fractional reduction at 850°C.

with appropriate boundary conditions. It is noted that only Eq. 6 or 7 need be considered, as the other can be obtained from the knowledge of the CO_2/CO ($=r$) ratio of the gas phase. The foregoing equations are recast in a dimensionless form as follows:

$$\frac{\partial^2\gamma}{\partial\sigma^2} + \phi^2\psi\left(\frac{\gamma}{1+\mu\gamma}\right) = 0 \tag{11}$$

$$\frac{\partial\psi}{\partial\tau} + \frac{\psi\gamma}{1+\mu\gamma} = 0 \tag{12}$$

where

$$\phi^2 = \frac{(2\beta-1)L^2RTI_1\rho_C^\circ}{D_2} \tag{13a}$$

$$\gamma = P_{CO_2}/P_{CO_2}^{(s)};\ \mu = IP_{CO_2}^{(s)} \tag{13b}$$

$$\psi = \rho_C/\rho_C^\circ;\ \sigma = y/L \tag{13c}$$

$$\tau = tM_CI_1P_{CO_2}^{(s)} \tag{13d}$$

The initial and boundary conditions stipulated earlier now become

$$\psi = 1 \text{ at } \tau = 0 \tag{14a}$$

$$\gamma = 1 \text{ at } \sigma = 1 \tag{14b}$$

$$(\partial\gamma/\partial\sigma) = 0 \text{ at } \sigma = 0 \tag{14c}$$

The foregoing system of equations pertains to carbon gasification and PbS-reduction processes. The PbS vaporization is treated separately. The progress of the overall reaction in the PbS:4CaO:4C mixture can be described in terms of the parameter $\bar{F}_C$, which is the fraction of solids converted to gas phase during the time interval τ. For the particular geometry (one-dimensional mass transfer) employed here, it can be shown that (Rao, 1974; Rao and Chuang, 1974)

$$\bar{F}_C = \int_0^1 (1-\psi)d\sigma \tag{15}$$

Accordingly, the weight of carbon removed from the sample during the time interval τ becomes

$$\Delta W_C = \bar{F}_C A_e L \rho_C^\circ \tag{16}$$

It will be noted that for each g-atom of carbon gasified, 2 g-moles of CO(g) are produced; of these 2β g-moles are utilized in the reduction of PbS(s). In other words, 2β g-atoms of oxygen are transferred to the gas phase albeit in the form of CO(g) and CO_2(g). The total weight loss due to the reduction (gasification inclusive) at time τ is given by

$$\Delta W_{red} = \bar{F}_C A_e L \rho_C^\circ[1 + (\beta M_{O_2}/M_C)] \tag{17}$$

The vaporization loss accompanying the reduction process can be calculated by considering Eq. 8 together with the appropriate boundary conditions. The phenomenon of PbS vaporization has been discussed in considerable detail elsewhere (El-Rahaiby and Rao, 1982); only the main result is presented here. The vaporization loss in time t is given by the following relationship:

$$\Delta W_{vap} = \frac{M_{PbS}D_3K_e\,\hat{\phi}\tanh\hat{\phi}A_e}{LRT}t \tag{18}$$

where M_{PbS} is the molecular weight of PbS, K_e is the equilibrium constant for vaporization (Kubaschewski and Alcock, 1979), t is time in seconds, and $\hat{\phi}$ is a dimensionless modulus defined as follows:

$$\hat{\phi} = L\hat{\alpha} \tag{19a}$$

$$\hat{\alpha} = (k_fRT/D_3K_e)^{1/2} \tag{19b}$$

The total weight loss resulting from reduction and vaporization phenomena is obtained by summation.

$$\Delta W_{cal} = \Delta W_{red} + \Delta W_{vap} \tag{20}$$

Application of the Model

The solution to the partial differential equations Eqs. 11 and 12 was obtained by the finite-difference method. The independent variables σ and τ are each subdivided into small intervals $\Delta\sigma$ and $\Delta\tau$, respectively. The following difference equations were derived in the usual manner:

$$\frac{\partial^2\gamma}{\partial\sigma^2} = \frac{\gamma_{i+1,j} - 2\gamma_{ij} + \gamma_{i-1,j}}{\Delta\sigma^2} \tag{21}$$

$$\frac{\partial\psi}{\partial\tau} = \frac{\psi_{i,j+1} - \psi_{ij}}{\Delta\tau} \tag{22}$$

Insertions into Eqs. 11 and 12 yield

$$\frac{\gamma_{i+1,j} - 2\gamma_{ij} + \gamma_{i-1,j}}{\Delta\sigma^2} + \phi^2\left(\frac{\psi_{ij}\gamma_{ij}}{1+\mu\gamma_{ij}}\right) = 0 \tag{23}$$

$$\frac{\psi_{i,j+1} - \psi_{ij}}{\Delta\tau} + \left(\frac{\psi_{ij}\gamma_{ij}}{1+\mu\gamma_{ij}}\right) = 0 \tag{24}$$

The last equation provides

$$\psi_{i,j+1} = \psi_{ij} - \Delta\tau\left(\frac{\psi_{ij}\gamma_{ij}}{1+\mu\gamma_{ij}}\right) \tag{25}$$

At $i = 0$, $\gamma_{1,j} = \gamma_{-1,j}$; boundary condition 14c

$$\gamma_{1,j} = \gamma_{0,j} - 0.5\Delta\sigma^2\phi^2\left(\frac{\psi_{0,j}\gamma_{0,j}}{1+\mu\gamma_{0,j}}\right) \tag{26a}$$

At $i \neq 0$

TABLE 2. EXPERIMENTAL AND CALCULATED DATA FOR THE CATALYZED REDUCTION UNDER He-RICH He-N_2 ATMOSPHERES

Run	T K	$r = \frac{CO_2}{CO}$	D_1 $cm^2 \cdot s^{-1}$	D_2 $cm^2 \cdot s^{-1}$	D_3 $cm^2 \cdot s^{-1}$	β	ρ_C° g C·cm^{-3}	k_f*	$P_{CO_2}^{(s)}$ Pa	μ	I_1
E113	1,061	13.38	2.2936	1.8215	0.9831	0.9570	0.134	4.392×10^{-10}	12.4	8.824×10^{-2}	1.85×10^{-3}
E114	1,083	7.66	2.4140	1.9111	1.0314	0.9292	0.134	9.859×10^{-10}	21.1	0.1459	2.65×10^{-3}
E108	1,101	4.45	2.2569	1.7902	0.9684	0.8896	0.145	2.001×10^{-9}	25.4	0.1910	4.28×10^{-3}
E107	1,138	1.85	2.5399	2.0215	1.0989	0.7977	0.137	6.698×10^{-9}	51.4	0.3780	7.74×10^{-3}
E109	1,161	1.18	2.4388	1.9440	1.0562	0.7424	0.146	1.511×10^{-8}	82.4	0.5586	1.17×10^{-2}
E110	1,190	0.71	2.5161	1.9989	1.0880	0.6804	0.138	3.565×10^{-8}	112.0	0.6654	1.46×10^{-2}
E111	1,212	0.50	2.6433	2.1066	1.1496	0.6418	0.144	7.191×10^{-8}	130.4	0.6951	2.08×10^{-2}
E112	1,247	0.25	2.9336	2.3421	1.2763	0.5822	0.137	1.914×10^{-7}	120.3	0.6383	2.69×10^{-2}

* k_f = mol·cm^{-3}·s^{-1}; I_1: mol·$(gC)^{-1}$·atm^{-1}·s^{-1}.

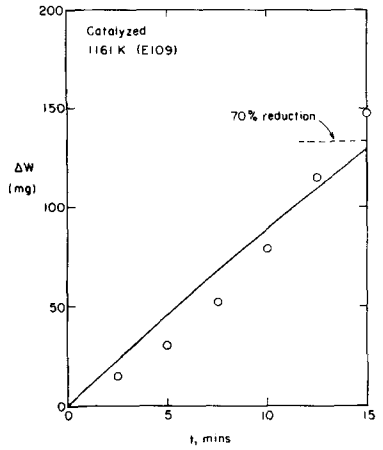

Figure 9. Fit between the experimental reduction kinetic data and the mathematical model at 1,161 K. Reduction carried out under helium-rich helium-nitrogen atmosphere.

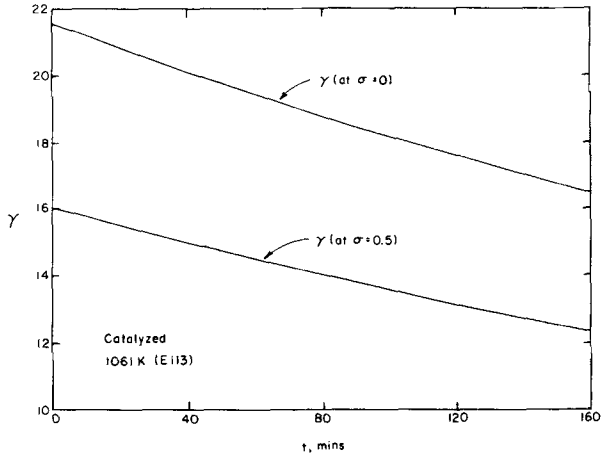

Figure 11. The variation of dimensionless CO_2 pressure (γ) with time at 1,061 K; reduction conducted under a helium-rich helium-nitrogen atmosphere.

$$\gamma_{i+1,j} = 2\gamma_{ij} - \gamma_{i-1,j} - \Delta\sigma^2\phi^2\left(\frac{\psi_{ij}\gamma_{ij}}{1+\mu\gamma_{ij}}\right) \qquad (26b)$$

The application of the model involves computing ΔW_{red} for an assigned value of the intrinsic rate constant I_1 and therefrom calculating ΔW_{cal} for the specified time interval t. The calculated value is then compared to the experimentally observed total weight loss for the time interval selected. The value of I_1 that gives the best fit is found by trial for each run.

The experimental ΔW vs. t data were correlated using this model. The first step in the data correlation concerned the evaluation of the vaporization contribution (ΔW_{vap}) to the observed weight loss. In general, this can be done by means of Eqs. 18 and 19. However, when computations were made using rate constant (k_f) values obtained from an earlier study (El-Rahaiby and Rao, 1982) on the vaporization into inert atmospheres, it was discovered that the vaporization term (ΔW_{vap}) was much too large. It is quite likely that the vaporization of PbS(s) in the presence of reactive gases like CO and CO_2 occurs more slowly than that under an inert gas. The modified k_f values for the vaporization loss of lead sulfide that occurs when the pore space gas phase contains CO(g) and CO_2(g) were deduced from the experimental data (Rao and El-Rahaiby, 1984).

These and other data used in the present calculations are listed in Table 2. The representative CO_2/CO ratio (r) for each temperature was determined by combining the galvanic cell data on r values obtained from the reduction experiments under pure helium and pure nitrogen atmospheres, respectively. Since there was some variation in the value of r with time, the representative value was taken as that near the 50% reduction mark. Furthermore, because the reduction process in the thermogravimetric apparatus was carried out in a He-N_2 atmosphere rather than in pure He, the corresponding r values were found by an interpolation based on

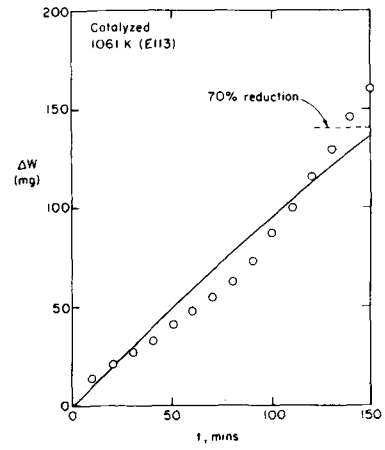

Figure 10. Fit between the experimental reduction kinetic data and the mathematical model at 1,061 K. Reduction carried out under helium-rich helium-nitrogen atmosphere.

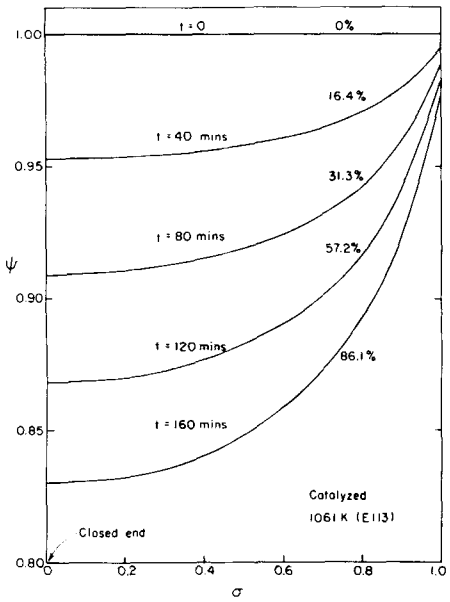

Figure 12. The profiles of dimensionless carbon mass concentration (ψ) at different time intervals in a PbS:4CaO:4C mixture reduced at 1,061 K under a helium-rich helium-nitrogen atmosphere. The percentages refer to extent of reduction.

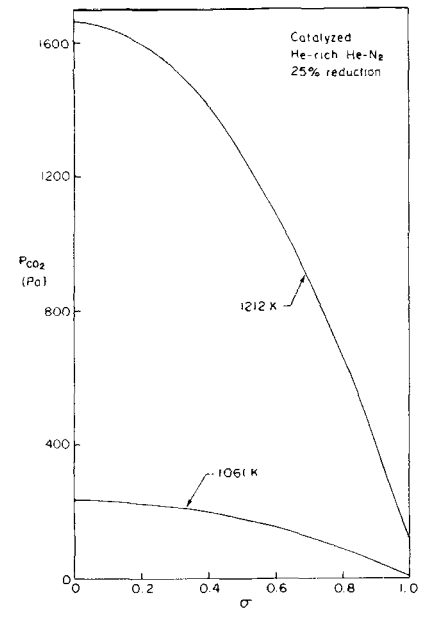

Figure 13. Profiles of CO_2 partial pressure in PbS:4CaO:4C mixtures reduced under a helium-rich helium-nitrogen atmosphere at 1,061 and 1,212 K, respectively.

the respective values for pure He and pure N_2 obtained from the galvanic cell experiments. At each temperature the utilization factor β was found by using the data on r and the effective diffusivities D_1 (for CO) and D_2 (for CO_2). It was found that β decreases with increasing temperature. The parameter I, defined in Eq. 9, was calculated using published data on I_2 and I_3 (Reif, 1952). The value of $P^{(s)}_{CO_2}$, the partial pressure of CO_2 in the gas phase near the exposed (upper) surface of the sample, was determined from

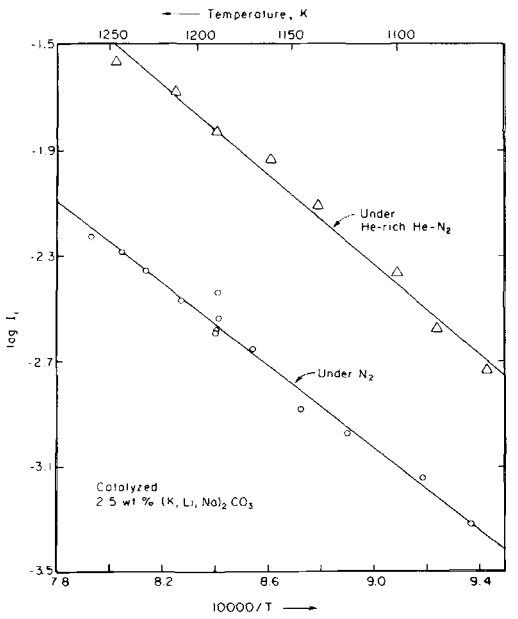

Figure 14. Arrhenius plots showing the temperature variation of the intrinsic rate constant (I_1) for reduction under a helium-rich helium-nitrogen atmosphere and a nitrogen atmosphere, respectively.

the reduction kinetic data and the gas flow rates as follows: The weight loss at time t, due to the reduction process alone, can be expressed as

$$\Delta W_{red} = 44n_{CO_2} + 28n_{CO} = n_{CO}(44r + 28) \quad (27)$$

where n_{CO} and n_{CO_2} are the moles of CO and CO_2 produced in time t. It follows that the production rates of CO and CO_2 are

$$f_{CO} = \frac{n_{CO}}{t} = \frac{\Delta W_{red}}{(44r + 28)t} \text{ and } f_{CO_2} = rf_{CO} \quad (28)$$

Furthermore

$$P^{(s)}_{CO} = f_{CO}(f_{CO} + f_{CO_2} + f_{N_2})^{-1} \text{ and } P^{(s)}_{CO_2} = rP^{(s)}_{CO} \quad (29)$$

where f_{CO}, f_{CO_2}, and f_{N_2} are the production (or flow) rates (in moles·min^{-1}) of CO, CO_2, and N_2, respectively. The method of calculation of the intrinsic rate constant I_1 using the analytical model, as detailed previously (Rao, 1974; Rao and Chuang, 1974), offers a useful insight into the present computation.

The fit between the model and the experimental ΔW vs. t data is shown in Figures 9 and 10; the agreement is reasonably good up to about 70% reduction. The variations of functions γ and ψ with σ and t for the catalyzed PbS:4CaO:4C sample reduced at 1,061 K (under He-rich He-N_2 atmosphere) were examined in some detail. The value of γ (at $\sigma = 0$), at the closed end, decreases with elapse of time, as shown in Figure 11; a similar behavior is observed with respect to γ (at $\sigma = 0.5$), at the midpoint in the reaction mixture. These trends simply mean that the reactive gases CO_2 and CO decline in concentration as the reduction progresses. The plots of the dimensionless mass concentration ($\psi = \rho_C/\rho^\circ_C$) of carbon vs. time are presented in Figure 12. It is seen that more carbon is gasified near the closed end than at the open end (or exposed surface) of the PbS:4CaO:4C sample. This is because of the greater retention of CO_2 at the closed end. The partial pressure profiles of CO_2 at two different temperatures (1,061 and 1,212 K) are shown in Figure 13. It is clear that the CO_2 concentration in the sample increases significantly as the temperature is raised.

The derived I_1 rate constant data for the He-rich He-N_2 runs are shown plotted according to the Arrhenius law in Figure 14. For the purpose of comparison, the I_1 data for reduction experiments under pure N_2 are also included. It is seen that the I_1 data for He-rich He-N_2 atmosphere are consistently greater than the corresponding data for pure N_2 atmosphere. The reasons for this behavior may now be considered. Since both He and N_2 are nonreactive atmospheres it is to be expected that the main difference between the two arises from the fact that the diffusivities D_1, D_2, and D_3 take on differing values in these two atmospheres. For instance, at 1061 K, the values of the effective diffusivities are found as follows.

With N_2 atmosphere: The binary diffusivities (for ordinary diffusion) of species CO, CO_2, and PbS in N_2 were found using the Chapman-Enskog relation (Bird et al., 1960). Since all three species are present in very dilute concentrations, ternary and higher order interactions can be neglected. It is seen that $D_{CO\text{-}N_2}$ is 1.76 cm^2·s^{-1} at 1,061 K. The effective diffusivity of CO in the porous mixture is determined using the following correlation (Weisz and Schwartz, 1962):

$$D_1 = D_{CO\text{-}N_2}(\theta^2/\sqrt{3}) \quad (30)$$

Substitutions yield $D_1 = 0.415$ cm^2·s^{-1} for CO in N_2. Similarly, we find $D_2 = 0.322$ cm^2·s^{-1} for CO_2 in N_2, and $D_3 = 0.163$ cm^2·s^{-1} for PbS in N_2, all at 1,061 K.

With He-rich He-N_2 atmosphere: The ordinary diffusivities for the pairs CO-He and CO-N_2 were found at first. Since the mole fraction of CO in the gas phase is exceedingly small, the term involving the ordinary diffusivity for the pair He-N_2 vanishes in the

final expression used for calculating the diffusivity of CO in the ternary CO-He-N_2 mixture (Bird et al., 1960). Thus,

$$D_{CO}^{ter} = 9.729 cm^2 \cdot s^{-1} \text{ at } 1{,}061K$$

The effective diffusivity D_1 is seen to be 2.294 $cm^2 \cdot s^-$ for CO. Similarly, D_2 = 1.822 $cm^2 \cdot s^{-1}$ for CO_2, and D_3 = 0.983 $cm^2 \cdot s^{-1}$ for PbS, all at 1061 K.

It is readily seen that the effective diffusivities of the species CO, CO_2, and PbS are much larger in the He-rich He-N_2 atmosphere as compared to those in the N_2 atmosphere. In applying the present mathematical model, proper allowance has been made for faster diffusion rates in the He-rich He-N_2 atmospheres. Despite this, there persisted a large difference between I_1 data for the He-rich He-N_2 runs and those for the pure N_2 runs.

This behavior may be contrasted with that noted in the study of vaporization of PbS from PbS:4CaO mixtures (El-Rahaiby and Rao, 1982). There, too, it was observed that vaporization under He-rich He-N_2 atmospheres proceeded considerably more rapidly than vaporization under pure N_2 atmosphere. But when the differences in the diffusivities were taken into account, the data lined up on a single Arrhenius plot, thus indicating that the kind of ambient atmosphere used has no real effect on the intrinsic rate constant (k_f) for vaporization, as long as the atmosphere is nonreactive. That the measured rates, which incorporate mass transfer influences in addition to the chemical kinetic factors, differed significantly did not pose a difficulty ultimately in interpreting the vaporization data satisfactorily. But the present data do not lend themselves to such an easy resolution.

In the PbS/CaO/C reaction system, we can identify at least two surface reaction processes, not counting the vaporization itself. The sulfide reduction step

$$PbS(s) + CaO(s) + CO(g) = Pb(l) + CaS(s) + CO_2(g) \quad (A1)$$

occurs at the lead sulfide/calcium oxide centers. The CO regeneration step

$$C(s) + CO_2(g) = 2CO(g) \quad (A2)$$

takes place at the carbon particle centers. The effect a nonreactive ambient atmosphere has on the course of these two reactions can only be understood if the intervening pore diffusion processes are taken into consideration. For instance, enhanced diffusion with a helium-containing He-N_2 medium will favor quicker transport of CO(g) to the PbS/CaO centers and a simultaneous fast transfer of CO_2(g) to C centers. The net effect will be a higher CO/CO_2 ratio in the pore space gas phase and a faster overall reduction. This is because the CO(g)-producing reaction A2 is greatly amenable to catalysis, whereas reaction A1 is practically unaffected by the catalysts like the alkali (K, Li, Na)$_2CO_3$ ternary. In such a situation (with CO and CO_2 constituting but a small fraction of the gas phase in the pore space), the rate of the reduction reaction A1 can be described by

$$\vec{r} = \vec{k}[(P_{CO}/P_{CO_2}) - (P_{CO}/P_{CO_2})_{eq}] \quad (31)$$

where P_{CO}/P_{CO_2} is the ratio in the gas phase near the PbS/CaO centers and $(P_{CO}/P_{CO_2})_{eq}$ is the equilibrium ratio for reaction A1. The faster this reaction proceeds, the greater is the rate of production of CO_2, which in turn diffuses to the C centers to react with them, producing more CO(g). Thus it will not be surprising if the derived rate constants for the two diffusing media (one is N_2 and the other is He-rich He-N_2) differ even after allowing for the enhanced diffusivity; the set under helium-containing atmosphere will be decidedly larger than that under N_2, all other conditions being the same. The fact that the gas species diffuse to the respective reaction centers more rapidly in a helium-containing gas mixture has consequences that cannot be explained by higher diffusivity alone. It is clear that in such a system the reactions have occurred to a greater extent (i.e., faster) because of the more favorable gas composition at the respective centers. This may be regarded as the synergistic effect. This occurs, perhaps to a small degree, in the uncatalyzed PbS/CaO/C system as well.

In the catalyzed PbS/CaO/C system, because of the rate enhancement induced in the Boudouard reaction by the alkali catalysts, the synergistic effect is greatly magnified. Thus the combined catalyst presence and He-rich He-N_2 atmosphere may be said to produce a synergistic effect as compared to the reaction carried out with the same catalyst but under a nitrogen atmosphere. This effect may be expressed quantitatively. The I_1 data shown in Figure 14 may be represented by the following relations, which were derived by the regression analysis of the data:

$$\log I_1(He) = 5.300 - \frac{162.37 kJ \cdot mol^{-1}}{2.303RT} \quad (32)$$

$$\log I_1(N_2) = 3.981 - \frac{149.16 kJ \cdot mol^{-1}}{2.303RT} \quad (33)$$

By comparing these two expressions, one may derive the value of the synergistic effect at any given temperature. For instance, it has values of 4.7 and 6.0 at 800 and 1,000°C, respectively. Thus, with increased temperature there is a slight gain in the synergistic effect.

ACKNOWLEDGMENT

The authors gratefully acknowledge the financial support of this work by the U.S. Department of Energy under contract No. DE-FC07-79CS40160. The authors also wish to thank H. G. Lee for his assistance.

NOTATION

A_e = area of cross section of the sample, cm^2
D_1 = effective diffusivity of CO, $cm^2 \cdot s^{-1}$
D_2 = effective diffusivity of CO_2, $cm^2 \cdot s^{-1}$
D_3 = effective diffusivity of PbS, $cm^2 \cdot s^{-1}$
$\overline{F}_C$ = fraction of the original carbon that has been gasified
f_i = production (or flow) rate of the ith species, $mol \cdot min^{-1}$
I = constant, $I_3 + (I_2/r)$, atm^{-1}
I_1 = intrinsic rate constant, $mol \cdot (gC)^{-1} \cdot atm^{-1} \cdot s^{-1}$
I_2 = adsorption rate coefficient, atm^{-1}
I_3 = adsorption rate coefficient, atm^{-1}
K = experimental rate constant, min^{-1}
$K(He)$ = experimental rate constant for He-rich He-N_2 atmosphere, min^{-1}
$K(N_2)$ = experimental rate constant for N_2 atmosphere, min^{-1}
K_e = equilibrium constant for vaporization of PbS(s)
k_f = forward rate constant for PbS-vaporization into reactive atmospheres, $mol \cdot cm^{-3} \cdot s^{-1}$
L = thickness of sample, cm
M_C = molecular weight of carbon
M_{O_2} = molecular weight of diatomic oxygen
M_{PbS} = molecular weight of PbS
n_i = moles of the ith species produced in time t
P_{CO} = partial pressure of CO at $y = y$, atm
P_{CO_2} = partial pressure of CO_2 at $y = y$, atm
P_{PbS} = partial pressure of PbS at $y = y$, atm

$P^{(s)}_{CO}$ = partial pressure of CO at the surface ($y = L$), atm
$P^{(s)}_{CO_2}$ = partial pressure of CO_2 at the surface ($y = L$), atm
q = D_1/rD_2
R = universal gas constant
r = CO_2/CO ratio in the gas phase
R_{CO} = net rate of formation of CO, mol·cm^{-3}·s^{-1}
R_{CO_2} = net rate of formation of CO_2, mol·cm^{-3}·s^{-1}
r_C = rate of carbon gasification, g·atom·(gC)$^{-1}$·s^{-1}
r_{CO} = rate of formation of CO by Boudouard reaction, mol·(gC)$^{-1}$·s^{-1}
s = synergistic effect
T = temperature, K
t = time, s
W°_T = initial weight of the PbS:4CaO:4C mixture, g
ΔW = weight loss sustained by the sample at time t, g
ΔW_C = weight of carbon gasified at time t, g
ΔW_{cal} = weight loss calculated by model at $t = t$, g
ΔW_{obs} = cumulative weight loss that corresponds to completion of reduction, g
ΔW_{red} = weight loss due to reduction at $t = t$, g
ΔW_{vap} = weight loss due to PbS vaporization at $t = t$, g
y = position coordinate, cm

Greek Letters

α = observed fractional reduction
$\hat{\alpha}$ = $(k_f RT/D_3K_e)^{1/2}$,cm^{-1}
β = utilization factor
γ = dimensionless pressure, $P_{CO_2}/P^{(s)}_{CO_2}$
μ = $IP^{(s)}_{CO_2}$
ρ_C = mass concentration of C in the mixture, gC·cm^{-3}
ρ°_C = initial mass concentration of C in the mixture, gC·cm^{-3}
σ = dimensionless positional coordinate, y/L
θ = void fraction or porosity
τ = dimensionless time, $tM_CI_1P^{(s)}_{CO_2}$
ϕ = dimensionless modulus, $[(2\beta - 1)L^2RT\, I_1\rho^\circ_C/D_2]^{1/2}$
ϕ = dimensionless modulus for PbS vaporization, $L\hat{\alpha}$
ψ = dimensionless carbon mass concentration, ρ_C/ρ°_C

LITERATURE CITED

Bird, R. B., W. E., Stewart, and E. N. Lightfoot, *Transport Phenomena*, Wiley, New York (1960).

El-Rahaiby, S. K., "Direct Reduction of Lead Sulfide with Carbon in the Presence of Lime (or Limestone)," Ph.D. Thesis, Univ. of Washington, Seattle (1983).

El-Rahaiby, S. K., and Y. K. Rao, "Kinetics of Vaporization of Lead Sulfide," *Metall. Trans. B*, **13B**, 633 (1982).

Kubaschewski, O., and. C. B. Alcock, *Metallurgical Thermochemistry*, 5th ed., Pergamon Press, Elmsford, NY (1979).

Rao, Y. K., "A Physico-Chemical Model for Reactions Between Particulate Solids occurring through Gaseous Intermediates. I. Reduction of Hematite by Carbon," *Chem. Eng. Sci.*, **29**, 1435 (1974).

Rao, Y. K., and Y. K. Chuang, "A Physico-Chemical Model for Reactions Between Particulate Solids occurring through Gaseous Intermediates. II. General Solutions," *Chem. Eng. Sci.*, **29**, 1933 (1974).

Rao, Y. K., and S. K. El-Rahaiby, "Direct Reduction of Lead Sulfide with Carbon and Lime; Effect of Catalysts." *Metall. Trans.* B, accepted for publication (1984).

Rao, Y. K., and B. P. Jalan, "A Study of the Rates of Carbon-Carbon Dioxide Reaction in the Temperature Range 839 to 1050°C," *Metall. Trans.*, **3**, 2465 (1972).

Reif, A. E., "The Mechanism of the Carbon Dioxide-Carbon Reaction," *J. Phys. Chem.*, **56**, 785 (1952).

Walker, Jr., P . L., F. Rusinko, Jr., and L. G. Austin, "Gas Reactions of Carbon," *Advan. Catal.*, **11**, 134, Academic Press, New York (1959).

Weisz, P. B., and A. B. Schwartz, "Diffusivity of Porous-Oxide-Gel-Derived Catalyst Particles," *J. Catal.*, **1**, 399 (1962).

Manuscript received Oct. 11, 1983; revision received Aug. 8, 1984, and accepted Aug. 17.